

Final Draft
of the original manuscript:

Matsumoto, H.; Ishiguro, T.; Konosu, Y.; Minagawa, M.; Tanioka, A.;
Richau, K.; Kratz, K.; Lendlein, A.:

**Shape-memory properties of electrospun non-woven fabrics
prepared from degradable polyesterurethanes containing
poly(Omega-pentadecalactone) hard segments**

In: European Polymer Journal (2012) Elsevier

DOI: 10.1016/j.eurpolymj.2012.07.008

Shape-Memory Properties of Electrospun Non-Woven Fabrics Prepared from Degradable Polyesterurethanes Containing Poly(ω -pentadecalactone) Hard Segments

Hidetoshi Matsumoto[†], Tasuku Ishiguro[†], Yuichi Konosu[†], Mie Minagawa[†], Akihiko Tanioka^{†},*

Klaus Richau[‡], Karl Kratz[‡], Andreas Lendlein[‡]

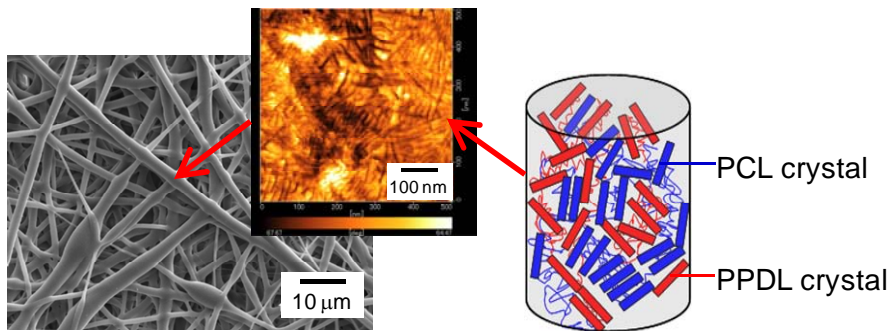
[†]Department of Organic and Polymeric Materials, and International Research Center of Macromolecular Science, Tokyo Institute of Technology, Mail Box S8-27, 2-12-1 Ookayama, Meguro-ku, Tokyo 152-8552, Japan

Tel: +81-3-5734-2426, Fax: +81-3-5734-2876, e-mail: tanioka.a.aa@m.titech.ac.jp

[‡]Centre of Biomaterial Development, Institute of Polymer Research and Berlin-Brandenburg Center for Regenerative Therapies, Helmholtz-Zentrum Geesthacht, Kantstrasse 55, D-14513 Teltow, Germany

Abstract Microscaled non-woven fabrics with fiber diameters in the range 1.8-3.1 μm were prepared by electrospinning from a chloroform solution of a degradable multiblock copolymer (PDLCL) consisting of crystallizable poly(ω -pentadecalactone) hard segments (PPDL) and poly(ε -caprolactone) switching segments (PCL). The surface morphology and microstructure of the non-woven fabrics were characterized by scanning electron microscopy, temperature-controlled scanning probe microscopy, wide angle X-ray diffraction (WAXD), and small angle X-ray scattering (SAXS). The microstructural analysis demonstrated that the rod-like domains of hard segment (PPDL) formed in the electrospun PDLCL fiber functioned as physical crosslinks. Cyclic, thermomechanical tensile tests showed that the

electrospun PDLCL fabrics exhibited good shape-memory properties with strain recovery rates of $R_r = 89-95\%$ and strain fixity rates of $R_f = 82-83\%$ after the 2nd cycle, when small deformations were applied at clinically relevant temperatures.



Graphical abstract for the table of contents

Keywords: electrospinning, thin fiber, shape-memory polymer, multiblock copolymer, degradable polymer

1. Introduction

Electrospinning is a straightforward and versatile method for forming continuous thin fibers based on an electrohydrodynamical process. This method has the following advantages: (i) applicability for a broad spectrum of molecules such as inorganic molecules, synthetic polymers, proteins, and DNA; and (ii) ability to produce thin fibers with diameters in the micrometer and nanometer range¹⁻⁶. Electrospun fibers or non-woven fabrics with large surface to volume ratio have recently attracted much attention for applications such as high-performance filter media, protective clothes, composites, drug delivery systems, and biomaterial scaffolds for tissue engineering^{2, 7-10}.

Shape-memory polymers (SMPs) possess the ability to memorize a permanent shape that can substantially differ from their temporary shape, the latter being obtained after a programming step. The transition from the temporary shape to the permanent one could be initiated by an external stimulus such as heat¹¹. Recently, in particular multifunctional SMPs combining at least two different functionalities

were intensively studied¹²⁻¹⁵ and have found growing interest in different application fields e.g. as smart textiles¹⁶ or medical devices^{17, 18}. In this context especially degradable SMPs are of particular interest for application in regenerative medicine approaches such as tissue engineering or induced auto-regeneration¹⁹⁻²⁸. Temperature-sensitive thermoplastic SMPs generally consist of two components on the molecular level: physical cross-links (hard segments) determining the permanent shape and switching segments fixing the temporary shape at temperatures below their thermal transition temperature T_{trans} ²⁹. Typical examples for such multifunctional thermoplastic SMPs are degradable linear multiblock copolymers exhibiting a phase-segregated morphology^{19-21, 25, 28}. Although, a broad variety of thermo-sensitive thermoplastic SMPs have been developed so far only a few reports address the investigation of electrospun fibers or structures thereof^{19, 30, 31}.

In the present study, we explored the shape-memory capability of electrospun non-woven fabrics prepared from degradable multiblock copolymers consisting of two crystallizable segments, poly(ω -pentadecalactone) hard segments (PPDL) and poly(ϵ -caprolactone) switching segments (PCL), which we named PDLCL. PDLCL was synthesised by the prepolymer method via co-condensation of two oligomeric PCL and PPDL macrodiols using an aliphatic diisocyanate as linker^{19, 20, 28, 32}. The aims of this study are (i) to prepare non-woven fabrics of PDLCL by electrospinning; and (ii) to characterize their morphology, internal microstructures, thermal properties, as well as their (iii) shape-memory properties. Here we examined the shape-memory capability of electro-spun PDLCL fabrics by applying small deformations (ϵ_m) ranging from 25% to 50%, where structural changes within the non-woven fabric (e.g. rearrangement of fiber orientation) should dominate the stress-strain behaviour. Additionally, in this work temperatures in the clinically relevant temperature range above body temperature up to 60 °C³³ were applied for programming and fixation of the temporary shape as well as for activation of the shape-memory effect (SME).

2. Experimental

2.1 Materials

PDLCL was prepared in two steps. First, the precursors were synthesized, which were then linked to the multiblock copolymers. For the synthesis of PPDL-diol 400 g ω -pentadecalactone (Geyer GmbH, Friedrichsthal, Germany, 97%) was dried under vacuum for 24 h. 19.5 g 1,8-Octanediol (Fluka, Taufkirchen, Germany, p.a., dried with 4 Å molecular sieve) and 75.7 mg dibutyltin oxide (Sigma-Aldrich, Taufkirchen, Germany, 98%; 90 ppm Sn) were added at 130 °C under N₂ atmosphere. The progress of the ring-opening polymerization was controlled by means of gel permeation chromatography (GPC). After the polymerization for 21 days, the reaction mixture was dissolved in THF (Fluka, Taufkirchen, Germany, p.a.) and poured into a large amount of an ethanol/water mixture (50/50 vol%) to precipitate the polymer. The poly(ω -pentadecalactone)diol was washed with ethanol (Berkel AHK, Berlin, Germany) and dried under vacuum at room temperature. The resulting poly(ω -pentadecalactone)diol was obtained in a yield of 93%.

Formatiert: Schriftartfarbe:
Automatisch

For synthesis of the multiblock copolymer according to the co-condensation method^{19,20}, 400 g of that PPDL-diol as telechelic precursor ($M_n^{app} = 4400 \text{ g}\cdot\text{mol}^{-1}$ and $T_m = 90 \text{ °C}$), 600 g PCL-diol ($M_n = 3000 \text{ g}\cdot\text{mol}^{-1}$ and $T_m = 43 \text{ °C}$, Solvay, Warrington, UK) and 4.4 g hexamethylene diisocyanate (HMDI, > 99%, Fluka, Taufkirchen, Germany) were reacted in toluene at 88 °C for 3 days using 160 mg dibutyltin laurate as catalyst. The product was obtained by precipitation in liquid nitrogen (yield 99%).

In order to determine the apparent molecular weight and polydispersity (PD), GPC measurements were performed on a system consisting of a PU-1580 pump (Jasco, Tokyo, Japan), 300 mm x 8 mm SDV columns-linear XL 10 μm (Polymer Standards Service GmbH, Mainz, Germany) as well as of an UV and a refractive index detector (Jasco, Tokyo, Japan). Chloroform (Acros Organics, Geel, Belgium) was used as eluent at a flow rate of 0.75 ml·min⁻¹ at ambient temperature. For evaluation of the data, the conventional calibration technique based on polystyrene standards with M_n between 1000 g·mol⁻¹ and 3000000 g·mol⁻¹ (Polymer Standards Service GmbH, Mainz, Germany) was used.

The copolymer composition was confirmed from the ratio of the ¹H-NMR PPDL signal at 1.25 ppm ($I_{CH_2,PPDL}$) and the PCL signal at 1.39 ppm ($I_{CH_2,PCL}$), recorded on a 500 MHz Bruker Avance

spectrometer (Karlsruhe, Germany) using deuterated chloroform as solvent and tetramethylsilane as internal standard. The PDDL weight content in wt% related to the starting composition of PDDL and PCL segments was calculated according to Eq. 1:

$$\frac{I_{CH_2,PPDL}(\delta = 1.25 ppm) / 20}{I_{CH_2,PCL}(\delta = 1.39 ppm) / 2} \cdot \frac{M_{n,PDL}(236)}{M_{n,CL}(114)} \cdot 100 = PDDL \text{ wt\%}, \quad (1)$$

$M_{n,PDL}$ and $M_{n,CL}$ being the number average molecular weights of the respective repeating units.

For the preparation of spinning solutions, chloroform (extra-pure grade, Wako, Osaka, Japan) was used as the solvent of PDLCL. PDLCL/chloroform solutions with concentrations ranging from 5 to 15 wt% were used. Organic solvent, pyridine (extra-pure grade, Wako, Osaka, Japan), was used as the additive for preparation of thinner fibers by electrospinning.

2.2 Electrospinning

The electrospinning device was the same as that used in a previous study³⁴. The polymer solution was contained in a syringe with a stainless steel nozzle (1.0 mm internal diameter). The nozzle was connected to a high-voltage regulated DC power supply (HDV-20K 7.5STD, Pulse Electronic Engineering, Noda, Japan). A constant volume flow rate was maintained via a syringe-type infusion pump (MCIP-III, Minato Concept, Tokyo, Japan). An aluminum plate (5 × 5 cm² area) was used as counter electrode. The distance between the nozzle tip and the counter electrode was 15 cm, the applied voltage was 15 kV, and the flow rates were 20 μl/min. The spun fibers were collected on the counter electrode to form a free-standing fabric with about 100 μm thickness. The electrospinning was carried out at 25 °C and at less than 20 % relative humidity.

2.3 Surface morphology, internal microstructure and thermal properties of PDLCL fabrics

The surface morphologies of the non-woven fabrics were observed using a scanning electron microscope (SEM, SM-200, Topcon, Tokyo, Japan) operated at 10 kV. All samples were sputter-coated with Au.

The surface morphology at 25 °C and 70 °C was characterized by a temperature controlled scanning probe microscope (SPM, Nanonavi E-sweep, SII Nanotechnology, Chiba, Japan) in the phase contrast mode.

Crystalline structures of PDLCL samples were investigated by wide angle X-ray diffraction (WAXD) measurements (RINT-2100 and RU-200, Rigaku, Akishima, Japan). WAXD intensity distribution as a function of the diffraction angle was measured using a diffractometer. The degree of crystallinity was evaluated as the ratio of the crystalline peak areas to the total area under the scattering curve.

Small angle X-ray scattering (SAXS) measurements were carried out using an instrument (Nanoviewer, Rigaku, Akishima, Japan) working at 40 kV and 20 mA with Ni-filtered CuK α radiation (wavelength of 0.15418 nm). The X-ray beam was collimated by a pinhole type slit. The two dimensional intensity data were detected using an imaging plate film (BAS-IP SR127, Fujifilm, Tokyo, Japan). The polymer sample and imaging plate film were set in a vacuum chamber to eliminate air scattering. The distance between sample and imaging plate film was 482 mm, and the exposure time was set to 120 min for each sample. The two dimensional intensity data were read with a RINT-RAXIS-DS3 scanner (Rigaku, Akishima, Japan). The one dimensional profiles in the scattering angle (2θ) range between 0.2 and 3 were obtained by averaging the two dimensional data. The long period was estimated from the one-dimensional correlation function ($\gamma_1(x)$) defined as:

$$\gamma_1(x) = \frac{\int_0^{\infty} s^2 I(s) \cos(2\pi xs) ds}{\int_0^{\infty} s^2 I(s) ds} \quad (2)$$

where $I(s)$, s , and x are the scattering intensity, the absolute value of the scattering vector ($=2\sin(\theta/\lambda)$), and the correlation length, respectively.

The thermal analysis of the non-woven fabrics was carried out using a differential scanning calorimeter (DSC, DSC6100, Seiko Instruments, Chiba, Japan). The samples were heated from 0 to 200 °C. All heating and cooling procedures were performed with a constant heating and cooling rate of 10 K·min⁻¹.

2.4 Shape-memory properties

The shape recovery rate R_r was used to quantify the ability of the material to regain its original shape²⁹. For a cycle N , R_r is calculated from the strain value of the temporary shape $\varepsilon_u(N)$ and the strain values of the tension-free states $\varepsilon_p(N)$ and $\varepsilon_p(N-1)$ of two subsequent cycles $N-1$ and N .

$$R_r(N) = \frac{\varepsilon_u(N) - \varepsilon_p(N)}{\varepsilon_u(N) - \varepsilon_p(N-1)} \quad (3)$$

The shape fixity rate R_f is defined as the quotient of the elongation $\varepsilon_u(N)$ in the tension-free state after cooling to T_{low} and the extension ε_m ²⁹.

$$R_f(N) = \frac{\varepsilon_u(N)}{\varepsilon_m} \quad (4)$$

R_f is a measure how well the material can fix the applied maximum deformation ε_m in the temporary shape.

In order to obtain information on relaxation and reorganisation in PDLCL non-wovens, cyclic thermomechanical measurements of the non-woven fabrics were performed by means of a thermomechanical analyser (TMA/SS6100, Seiko Instruments, Chiba, Japan). PDLCL as-spun fabrics were cut into rectangular stripes with dimension of $1.5 \times 15.0 \times 0.1 \text{ mm}^3$.

Each cycle consisted of a multi-step programming module (i, ii), where the temporary shape is created, and a recovery module (iii) where the original shape is recovered. Every recovery module is completed by a waiting period of 10 minutes.

Two different kinds of cyclic thermomechanical measurements were applied: In method (A) a low maximum strain of $\varepsilon_m = 25\%$ was applied, which was constant for all five subsequent cycles, while during method (B) ε_m was increased as in the four subsequent cycles from 25% to 35% to 50% (cycles 3 and 4). The extension rate was 1.25 mm/min in all experiments with fabrics.

For programming the test stripe of the non-woven fabric was heated to a temperature $T_{prog} = T_{high} = 60 \text{ }^\circ\text{C}$ (which was above the melting temperature of the PCL switching segments $T_{m,PCL} = 53 \text{ }^\circ\text{C}$

obtained from DSC analysis) and stretched to ε_m (i). Then the sample was kept at 60 °C for 10 min to allow relaxation and afterwards cooled down to the fixation temperature $T_{low} = 40$ °C ($< T_{m,PCL} = 53$ °C) under a constant extension ε_m and is unloaded to 0 % stress at 40 °C. Finally the stress is removed. The observed elongation of the sample in the temporary state is ε_u (ii). Afterwards for recovery under stress-free conditions the sample was heated to a temperature $T_{high} = 60$ °C ($> T_{m,PCL} = 53$ °C but below the onset of the T_m of the PDDL segments). While heating the sample contracts (the permanent shape is recovered), giving the strain value of the tension-free state ε_p .

3. Results and Discussion

3.1 Characterization of PDLCL

The apparent number average molecular weight obtained for the synthesized multiblock copolymer PDLCL was $M_n^{app} = 65000$ g·mol⁻¹, with a polydispersity of PD = 2.2. The calculated PDDL weight content of 41 wt% determined by ¹H-NMR corresponds well to the reaction ratio of the poly(ϵ -caprolactone)diol and poly(ω -pentadecalactone)diol in the starting material mixture.

3.2 Characterization of non-woven PDLCL fabrics

To identify the optimal conditions for the fiber formation, PDLCL fabrics were created by electrospinning from polymer solutions of various polymer concentrations (5-15 wt%). Fig. 1 shows the surface SEM images of the achieved non-woven fabrics. All solutions showed good processability below 15 wt% polymer content, whereby the fiber diameter increased with increasing polymer concentration of the solution. At higher concentration above 15 wt%, on the other hand, the jet was not stable and the polymer solution often clogged up at the tip of nozzle. A smooth fibrous structure without beads was formed above 12.5 wt%. In general, the addition of electrolytes to the spinning solution increases the solution conductivity and enhances the formation of the field-induced electric charges causing electrostatic repulsion on the surface of the jet. This effect allows the forming of thin and homogeneous fibers by electrospinning³⁵. We used pyridine as organic electrolyte. The advantage of

Gelöscht: 2

the organic electrolyte, such as pyridine, is that it is evaporated during electrospinning and does not remain in the resulting fiber. The addition of pyridine was effective for forming thin fibers (Fig. 1f-h). We used the fabrics with comparatively narrow fiber diameter distribution, which were created from the 15 wt% solution containing 10 wt% of pyridine, for the thermomechanical measurements and other characterizations.

The thermal properties of the non-woven PDLCL fabrics were investigated by DSC. The DSC thermogram showed two melting peaks with a maximum around 53 °C and 85 °C (Fig.2). The peak around 53 °C was attributed to the melting point ($T_{m,PCL}$) of crystallites of the PCL phase and that at 85 °C to the $T_{m,PPDL}$ of the crystallites of the PPDL phase²⁰.

To investigate the internal microstructure of the PDLCL fabric, WAXD and SAXS measurements were carried out. Fig. 3a shows the X-ray diffraction profile of the electrospun PDLCL fabric, where two diffraction peaks at 21.4 and 23.9 degrees were observed. WAXD was mainly applied for determination of the overall degree of crystallinity (DOC) PDLCL as the two segments of the multiblock copolymer PCL and PPDL exhibit an isomorphous crystal structure³⁶⁻⁴⁰. The degree of crystallinity of the PDLCL fabric calculated by the WAXD data was 24%. This value is lower than the values of as-received PDLCL in the range of 33-39%²⁰. This difference can be explained by the rapid solidification during electrospinning, which does not allow sufficient time for copolymer blocks to reach their equilibrium morphologies⁴¹.

Fig.3b shows the small angle X-ray scattering curve of the PDLCL fabric. A weak scattering peak was observed. Fig.3c shows the one-dimensional correlation function ($\gamma_1(x)$) obtained from the scattering profile. The long period of periodic structures in the as-spun PDLCL estimated from the correlation function was 10 nm. These periodic structures are discussed further in the following paragraph 3.3.

3.3 Shape-memory properties

The shape-memory capability of the PDLCL non-woven fabrics was explored by conducting cyclic, thermomechanical tensile tests, using clinically relevant temperatures for deformation, fixation and recovery. While in test method (A) a constant deformation of $\varepsilon_m = 25\%$ was applied in each cycle in method (B) ε_m was increased in subsequent cycles from 25% to 50%. Fig. 4 shows the obtained strain-stress curves of the cyclic thermomechanical measurements and the calculated R_f and R_r values, relaxed stress, and Young's moduli are summarized in Table 1. The Young's moduli at 40 °C were larger than those at 60 °C. This is due to the coexistence of the crystallites of PPDL and PCL phases in the fabrics at 40 °C (At 60 °C, crystallites of PCL phase melted and only the crystallites of PPDL phase existed in the fabrics). R_r obtained in test method (A) varied significantly between the first and the second cycle, whereas the following cycles are similar to the results of the second cycle with $R_r \geq 89\%$. In contrast R_f was found to be constant around $R_f = 83\%$ for all cycles. The difference is commonly observed in such cyclic tests and it is attributed to the molecular-scaled reorganization of polymer accompanied with deformation of the sample (i.e., the break of the crosslinks mentioned previously)⁴². This showed that the electrospun PDLCL fabrics have well reproducible shape-memory properties, when a relatively small extension and clinically relevant temperatures of $T_{prog} = T_{high} = 60$ °C and $T_{low} = 40$ °C were applied. In contrast, when ε_m was increased from 25% to 50% in test method (B) R_r could not reach the values of the aforementioned experiments with constant $\varepsilon_m = 25\%$ after the second cycle. As shown in Fig. 4b, the stress increased linearly until the point that strain reached the value of the previous cycle, and then the relaxation of stress occurred. This resulted in the decrease in the recovery rates.

To discuss the mechanisms of the SME based on deformation of the internal microstructures of the PDLCL fabrics, first we have to consider the effect of macroscopic structural change of the fabric with a fibrous network structure (Fig. 5a). After the first programming and recovery process, the macroscopic change of the fabric structure was observed (Fig. 5b). During the following cycles the macroscopic structure of the deformed non-woven fabric remains unchanged. For comparison, we prepared the aligned PDLCL fabric prepared by electrospinning with rotating collector (Fig. 5c) and then characterized the shape-memory properties. The recovery rate is almost same to that of non-aligned

Formatiert: Schriftartfarbe:
Automatisch

Formatiert: Schriftartfarbe:
Automatisch

Formatiert: Schriftartfarbe:
Automatisch

fabric (Table S1). These results supported that the shape-memory properties were substantially determined by the internal structures of multiblock copolymers, but not by macroscopic structural changes within the non-woven fabric.

Formatiert: Schriftartfarbe:
Automatisch

Gelöscht:

To elucidate the relationship between the shape-memory properties and the internal microstructure of the as-spun fabrics, the surface morphology at 25 and 70 °C was characterized by SPM. The samples were heated from 25 to 70 °C and then cooled to 25 °C. These temperatures were chosen from the DSC results (Fig. 2) according to the temperature interval of $T_{m,PCL}$ and well below the onset of $T_{m,PPDL}$, in order to be able to observe the SPM phase contrast differences between PCL and PPDL domains. Fig. 6 shows the SPM phase contrast images of the non-woven PDLCL fabrics at different temperatures. The rod-like structures, where the phase lag was relatively small, were observed on the surface of the fibers at room temperature (Fig. 6a). At 70 °C, half of the rods disappeared (Fig. 6b), and after recooling to room temperature, they appeared again (Fig. 6c). The average distance between two rod-like structures displayed in Fig. 6a was 10 nm. This value corresponds exactly to the long period calculated from the SAXS measurement mentioned earlier. Therefore we can conclude that these structures originate from crystal regions in the fiber schematically shown in Fig. 6d. When the electrospun fiber was heated, the rod-like structures of the crystalline PCL switching domains melted and the fiber became more elastic because of the gained mobility of PCL segment. After cooling, the rod-like structure (PCL crystal) appeared again. These results supported the hypothesis that the rod-like domains of hard segments (PPDL crystals) formed in electrospun PDLCL fabrics functioned as physical crosslinks. Interestingly, such rod-like structures could not be observed on the surface of solvent-casted and spin-coated PDLCL films (Fig.S1).

As mentioned above, the relaxation of stress during programming caused the decrease in the recovery rates when test method B with increasing ϵ_m -values was applied (Fig. 4b). Now this can be attributed to the rearrangement of the polymer chains including the hard segments in the fiber, as evidenced by the SPM image of the surface of the electrospun PDLCL fiber after programming (elongated at T_{high} , Fig. 6e). The rod-like structures were aligned along the fiber axis. In the recovery process, the oriented

switching segments of PCL shrink after reheating by entropy driven recoiling. The aligned rod-like domains of crystallized hard segments (PPDL crystal), however, cannot recover the original structure.

This rearrangement also influenced the Young's modulus at 40 °C for test method B, which showed the cycle number-dependent decrease.

Formatiert: Schriftartfarbe:
Automatisch

4. Conclusions

Non-woven fabrics based on degradable multiblock copolymer (PDLCL) were prepared by electrospinning. The average diameter of the fibers in the fabrics ranged from 1.8 to 3.1 μm . The electrospun PDLCL multiblock copolymer showed good shape-memory properties with strain recovery rates of 89-95% and strain fixity rates of 82-83% after the 2nd cycle, when small deformations were applied at clinically relevant temperatures.

The SPM observation and SAXS measurement revealed that the electrospun PDLCL multiblock copolymer contained rod-like structures, which originated from the crystalline domains of the copolymer in the fiber. The rod-like crystalline structures of PPDL worked as physical crosslinks up to 70 °C, which is below the onset of $T_{m,PPDL}$. These structures could not be seen in PDLCL samples obtained by other processes (i.e., cast and spin-coated films), but they became aligned along the fiber axis after programming at 60 °C. Therefore we hypothesize that the variation of the characteristic dimension (e.g. fiber diameter) of semi-crystalline SMPs can be a promising tool to systematically influence the arrangement and reorganisation of crystalline structures during programming and recovery and in this way the shape-memory capability.

ACKNOWLEDGMENTS. The authors are grateful to Associate Professor Shigeo Asai and Professor Mitsuru Ueda, Tokyo Institute of Technology, for the X-ray analyses (WAXD and SAXS) and TMA measurements, respectively. The authors thank Dr. Michael Zierke, HZG, for synthesis of the polymer sample and Ms. Mari Yamamoto as well as Mr. Yukiya Watanabe, SII Nanotechnology, for the scanning probe microscope observations.

REFERENCES

1. Dzenis, Y., Spinning Continuous Fibers for Nanotechnology. *Science* **2004**, 304, (5679), 1917-1919.
2. Greiner, A.; Wendorff, J. H., Electrospinning: A fascinating method for the preparation of ultrathin fibres. *Angewandte Chemie-International Edition* **2007**, 46, (30), 5670-5703.
3. Li, D.; Xia, Y., Electrospinning of Nanofibers: Reinventing the Wheel? *Advanced Materials* **2004**, 16, (14), 1151-1170.
4. Reneker, D. H.; Chun, I., Nanometre diameter fibres of polymer, produced by electrospinning. *Nanotechnology* **1996**, 7, (3), 216-223.
5. Reneker, D. H.; Yarin, A. L.; Zussman, E.; Xu, H., Electrospinning of nanofibers from polymer solutions and melts. In *Advances in Applied Mechanics, Vol 41*, 2007; Vol. 41, pp 43-195.
6. Nakashima, K.; Tsuboi, K.; Matsumoto, H.; Ishige, R.; Tokita, M.; Watanabe, J.; Tanioka, A., Control over Internal Structure of Liquid Crystal Polymer Nanofibers by Electrospinning. *Macromolecular Rapid Communications* **2010**, 31, (18), 1641-1645.
7. Agarwal, S.; Wendorff, J. H.; Greiner, A., Progress in the Field of Electrospinning for Tissue Engineering Applications. *Advanced Materials* **2009**, 21, (32-33), 3343-3351.
8. Huang, C.; Soenen, S. J.; Rejman, J.; Lucas, B.; Braeckmans, K.; Demeester, J.; De Smedt, S. C., Stimuli-responsive electrospun fibers and their applications. *Chemical Society Reviews* **2011**, 40, (5), 2417-2434.
9. Lannutti, J.; Reneker, D.; Ma, T.; Tomasko, D.; Farson, D. F., Electrospinning for tissue engineering scaffolds. *Materials Science & Engineering C-Biomimetic and Supramolecular Systems* **2007**, 27, (3), 504-509.
10. Lu, P.; Ding, B., Applications of Electrospun Fibers. *Recent Patents on Nanotechnology* **2008**, 2, 169-182.
11. Behl, M.; Zotzmann, J.; Lendlein, A., Shape-Memory Polymers and Shape-Changing Polymers. *Advances in Polymer Science* **2010**, 226, 1-40.
12. Behl, M.; Razzaq, M. Y.; Lendlein, A., Shape-Memory Polymers: Multifunctional Shape-Memory Polymers *Advanced Materials* **2010**, 22, (31), 3388-3410.
13. Mather, P. T.; Luo, X.; Rousseau, I. A., Shape Memory Polymer Research. *Annual Review of Materials Research* **2009**, 39, 445-71.
14. Rousseau, I. A., Challenges of Shape Memory Polymers: A Review of the Progress Toward Overcoming SMP's Limitations. *Polymer Engineering and Science* **2008**, 48, (11), 2075-2089.
15. Xie, T., Recent advances in polymer shape memory. *Polymer* **2011**, 52, (22), 4985-5000.
16. Hu, J.; Chen, S., A review of actively moving polymers in textile applications. *Journal of Materials Chemistry* **2010**, 20, (17), 3346-3355.
17. Lendlein, A.; Behl, M.; Hiebl, B.; Wischke, C., Shape-memory polymers as a technology platform for biomedical applications. *Expert Review of Medical Devices* **2010**, 7, (3), 357-379.

18. Small, I. V. W.; Singhal, P.; Wilson, T. S.; Maitland, D. J., Biomedical applications of thermally activated shape memory polymers. *Journal of Materials Chemistry* **2010**, 20, (17), 3356-3366.
19. Kratz, K.; Habermann, R.; Becker, T.; Richau, K.; Lendlein, A., Shape-memory properties and degradation behavior of multifunctional electro-spun scaffolds. *Int J Artif Organs* **2011**, 34, (2), 225-230.
20. Kratz, K.; Voigt, U.; Wagermaier, W.; Lendlein, A., Shape-memory properties of multiblock copolymers consisting of poly(ω -pentadecalactone) hard segments and crystallizable poly(ϵ -caprolactone) switching segments. *Mater. Res. Soc. Symp. Proc.* **2008**, 1140, 17-22.
21. Lendlein, A.; Langer, R., Biodegradable, elastic shape-memory polymers for potential biomedical applications. *Science* **2002**, 296, (5573), 1673-1676.
22. Nagahama, K.; Ueda, Y.; Ouchi, T.; Ohya, Y., Biodegradable Shape-Memory Polymers Exhibiting Sharp Thermal Transitions and Controlled Drug Release. *Biomacromolecules* **2009**, 10, (7), 1789-1794.
23. Schneider, T.; Kohl, B.; Sauter, T.; Becker, T.; Kratz, K.; Schossig, M.; Hiebl, B.; Jung, F.; Lendlein, A.; Ertel, W.; Schulze-Tanzil, G., Viability, Adhesion and Differentiated Phenotype of Articular Chondrocytes on Degradable Polymers and Electro-Spun Structures Thereof. *Macromolecular Symposia* **2011**, 309-310, (1), 28-39.
24. Serrano, M. C.; Carbajal, L.; Ameer, G. A., Shape-Memory Polymers: Novel Biodegradable Shape-Memory Elastomers with Drug-Releasing Capabilities (Adv. Mater. 19/2011). *Advanced Materials* **2011**, 23, (19), 2210-2210.
25. Wang, Y.; Li, Y.; Luo, Y.; Huang, M.; Liang, Z., Synthesis and characterization of a novel biodegradable thermoplastic shape memory polymer. *Materials Letters* **2009**, 63, (3-4), 347-349.
26. Wischke, C.; Neffe, A. T.; Steuer, S.; Lendlein, A., Evaluation of a degradable shape-memory polymer network as matrix for controlled drug release. *Journal of Controlled Release* **2009**, 138, (3), 243-250.
27. Zotzmann, J.; Behl, M.; Hofmann, D.; Lendlein, A., Reversible Triple-Shape Effect of Polymer Networks Containing Poly(ω -pentadecalactone)- and Poly(ϵ -caprolactone)-Segments. *Advanced Materials* **2010**, 22, (31), 3424-3429.
28. Feng, Y. K.; Behl, M.; Kelch, S.; Lendlein, A., Biodegradable Multiblock Copolymers Based on Oligodepsipeptides with Shape-Memory Properties. *Macromolecular Bioscience* **2009**, 9, (1), 45-54.
29. Wagermaier, W.; Kratz, K.; Heuchel, M.; Lendlein, A., Characterization Methods for Shape-Memory Polymers. *Advances in Polymer Science* **2010**, 226, 97-145.
30. Cha, D. I.; Kim, H. Y.; Lee, K. H.; Jung, Y. C.; Cho, J. W.; Chun, B. C., Electrospun nonwovens of shape-memory polyurethane block copolymers. *Journal of Applied Polymer Science* **2005**, 96, (2), 460-465.
31. Zhuo, H.; Hu, J.; Chen, S., Electrospun polyurethane nanofibres having shape memory effect. *Materials Letters* **2008**, 62, (14), 2074-2076.
32. Grablowitz, H.; Lendlein, A., Synthesis and characterization of alpha, omega-dihydroxy-telechelic oligo(p-dioxanone). *Journal of Materials Chemistry* **2007**, 17, (38), 4050-4056.
33. Small, W.; Wilson, T. S.; Bennett, W. J.; Loge, J. M.; Maitland, D. J., Laser-activated shape memory polymer intravascular thrombectomy device. *Optics Express* **2005**, 13, (20), 8204-8213.
34. Matsumoto, H.; Wakamatsu, Y.; Minagawa, M.; Tanioka, A., Preparation of ion-exchange fiber fabrics by electrospray deposition. *Journal of Colloid and Interface Science* **2006**, 293, (1), 143-150.
35. Yarin, A. L.; Koombhongse, S.; Reneker, D. H., *Taylor cone and jetting from liquid droplets in electrospinning of nanofibers*. AIP: 2001; Vol. 90, p 4836-4846.
36. Bittiger, H.; Marchessault, R. H.; Niegisch, W. D., Crystal structure of poly- ϵ -caprolactone. *Acta Crystallographica Section B* **1970**, 26, (12), 1923-1927.
37. Cai, J.; Hsiao, B. S.; Gross, R. A., Real-Time Structure Changes during Uniaxial Stretching of Poly(ω -pentadecalactone) by in Situ Synchrotron WAXD/SAXS Techniques. *Macromolecules* **2011**, 44, (10), 3874-3883.

38. Ceccorulli, G.; Scandola, M.; Kumar, A.; Kalra, B.; Gross, R. A., Cocrystallization of Random Copolymers of ϵ -Pentadecalactone and μ -Caprolactone Synthesized by Lipase Catalysis. *Biomacromolecules* **2005**, 6, (2), 902-907.
39. Gazzano, M.; Malta, V.; Focarete, M. L.; Scandola, M.; Gross, R. A., Crystal structure of poly(ω -pentadecalactone). *Journal of Polymer Science Part B: Polymer Physics* **2003**, 41, (10), 1009-1013.
40. Pan, P.; Inoue, Y., Polymorphism and isomorphism in biodegradable polyesters. *Progress in Polymer Science* **2009**, 34, (7), 605-640.
41. Ma, M.; Hill, R. M.; Lowery, J. L.; Fridrikh, S. V.; Rutledge, G. C., Electrospun Poly(Styrene-block-dimethylsiloxane) Block Copolymer Fibers Exhibiting Superhydrophobicity. *Langmuir* **2005**, 21, (12), 5549-5554.
42. Lendlein, A.; Schmidt, A. M.; Langer, R., AB-polymer networks based on oligo(ϵ -caprolactone) segments showing shape-memory properties. *Proceedings of the National Academy of Sciences of the United States of America* **2001**, 98, (3), 842-847.

Table 1

The strain recovery rate (R_r) and fixity rate (R_f) obtained from the cyclic thermomechanical measurements of PDLCL non-woven fabrics. (fixed programming parameters $T_{prog} = 60$ °C, $T_{low} = 40$ °C and $T_{high} = 60$ °C)

Cycle No.	Method A					Method B						
	ϵ_m [%]	$R_f(N)$ [%]	$R_r(N)$ [%]	Relaxed stress [MPa]	Young's modulus		ϵ_m [%]	$R_f(N)$ [%]	$R_r(N)$ [%]	Relaxed stress [MPa]	Young's modulus	
					[MPa]						[MPa]	
					40°C	60°C					40°C	60°C
1	25	83	58	0.064	7.8	3.6	25	92	49	0.084	21.2	2.7
2	25	82	89	0.056	8.0	3.6	35	92	76	0.11	19.5	3.3
3	25	82	93	0.057	7.9	3.6	50	93	80	0.14	17.8	3.3
4	25	83	95	0.053	7.8	3.6	50	-	-	-	-	3.4

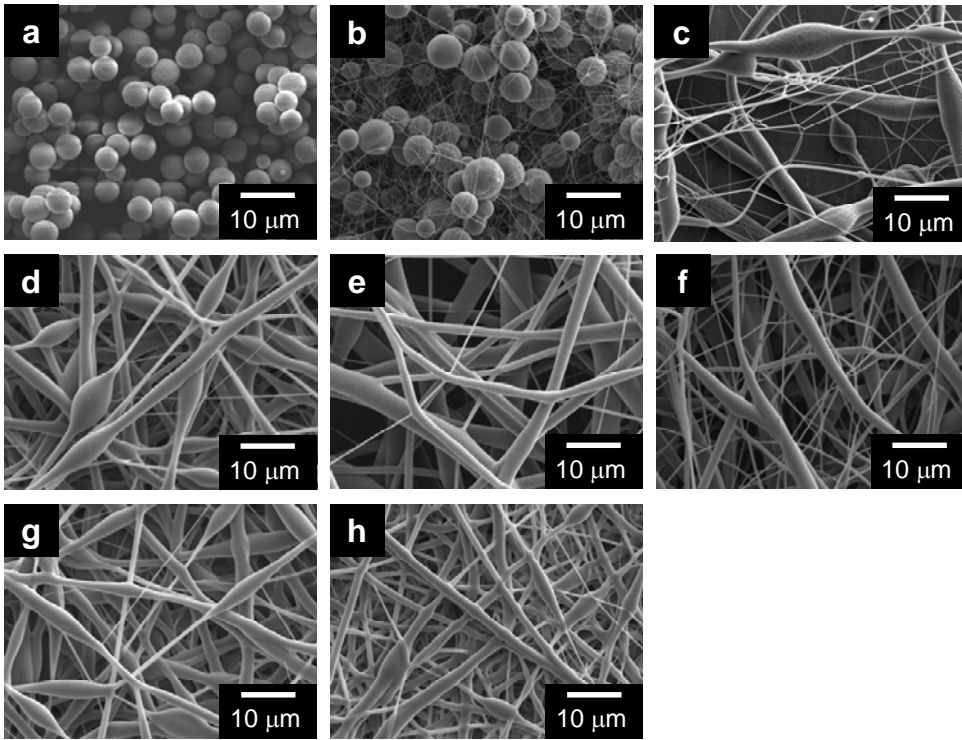


Figure 1. Surface SEM images of the electrospun fabrics from PDLCL/chloroform solutions with various polymer concentrations: (a) 5 wt%; (b) 7.5 wt%; (c) 10 wt%; (d) 12.5 wt%; (e) 15 wt% (f) 15 wt% containing 1 wt% of pyridine; (g) 15 wt% containing 5 wt% of pyridine; (h) 15 wt% containing 10 wt% of pyridine. The average fiber diameters were; (b) $0.2 \pm 0.1 \mu\text{m}$; (c) $0.7 \pm 1.2\mu\text{m}$; (d) $1.2 \pm 0.4\mu\text{m}$; (e) $3.1 \pm 1.3 \mu\text{m}$; (f) $2.7 \pm 1.2 \mu\text{m}$; (g) $2.7 \pm 1.0 \mu\text{m}$; (h) $1.8 \pm 0.4 \mu\text{m}$, which were determined by SEM image analysis using Adobe Photoshop software (CS4 Extended, San Jose, USA).

Gelöscht: .
 Formatiert: Schriftartfarbe: Automatisch

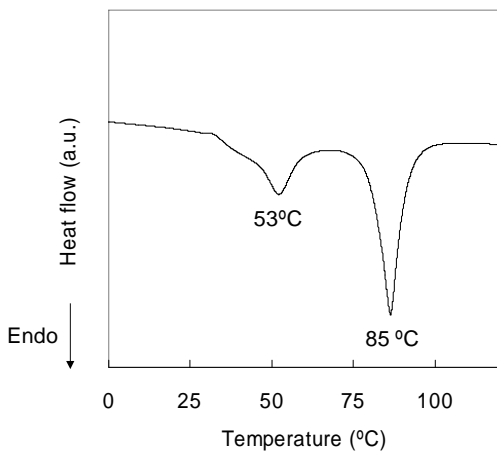


Figure 2. DSC thermogram obtained from the first heating run for PDLCL non-wovens.

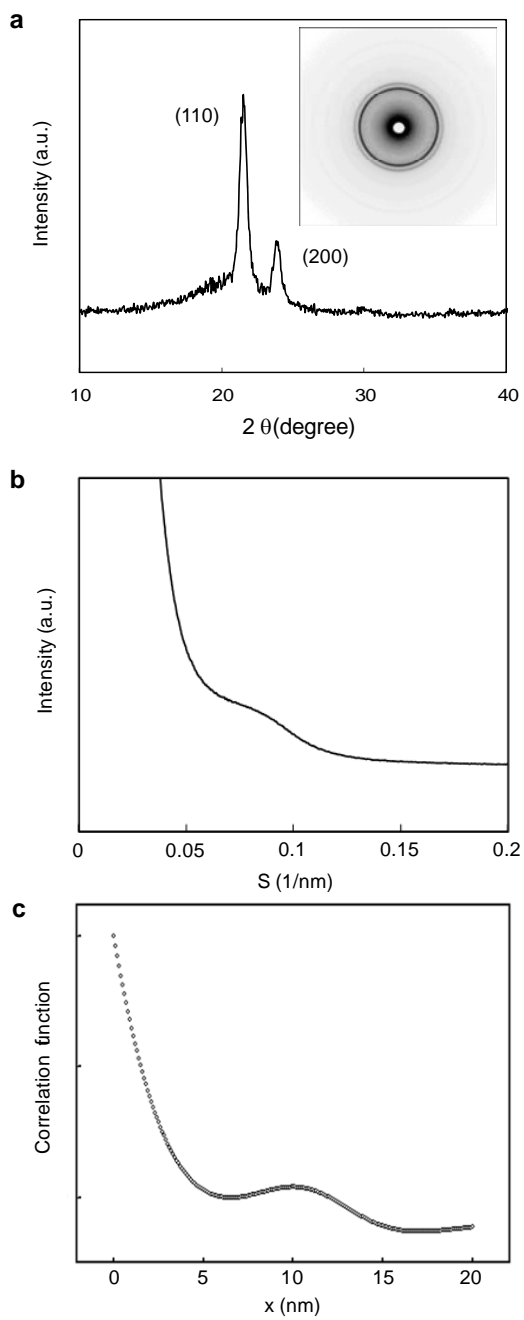


Figure 3. (a) WAXD and (b) SAXS profiles of non-woven PDLCL fabrics obtained at ambient temperature. (c) Correlation function obtained by SAXS data.

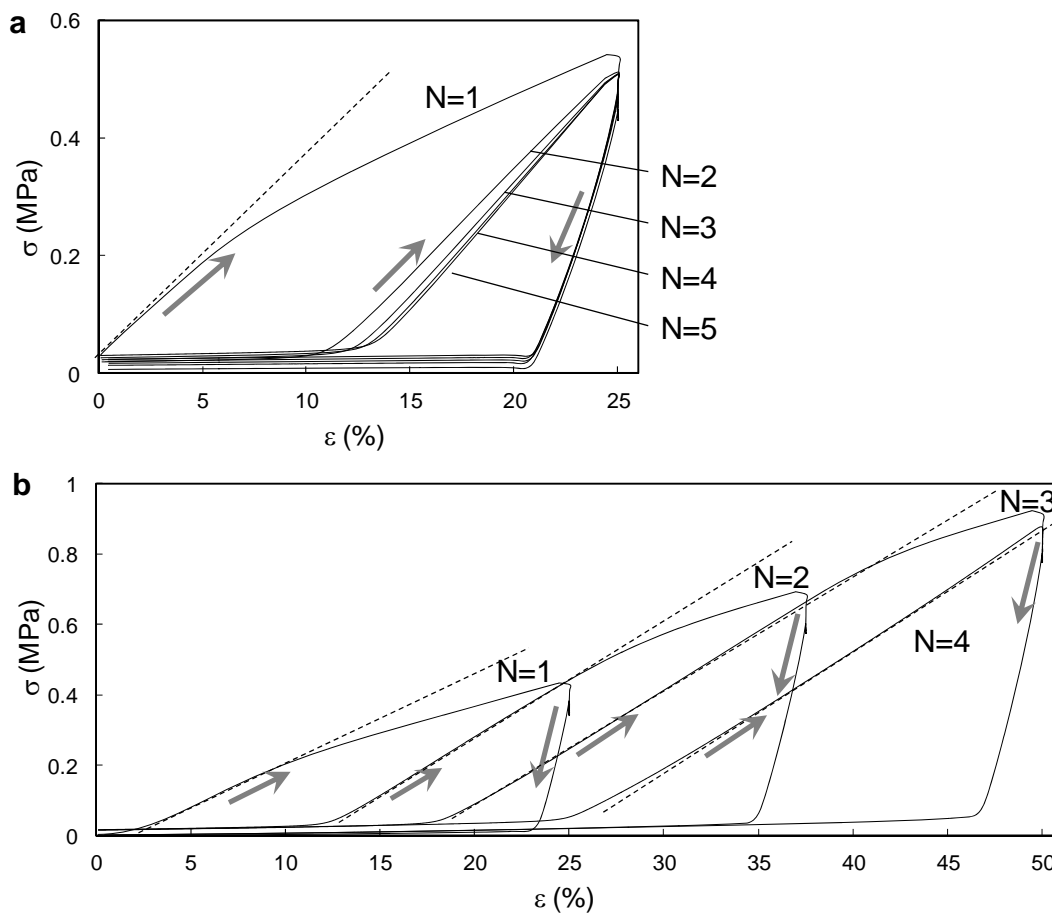


Figure 4. Strain-stress curves of PDLCL non-wovens obtained by the cyclic thermomechanical measurements with $T_{prog} = T_{high} = 60$ °C and $T_{low} = 40$ °C. Method A: five subsequent cycles with $\epsilon_m = 25\%$ (a) and Method B: four subsequent cycles with increasing ϵ_m from 25% to 50% (b). The inserted dashed lines indicate the linear regression applied for calculation of the Young's modulus.

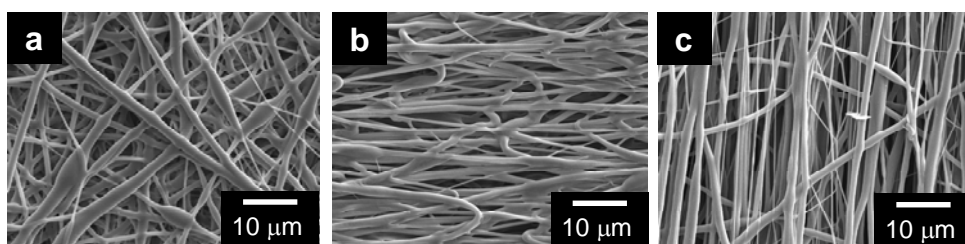


Figure 5. SEM images of as-spun PDLCL multiblock copolymer (a) before and (b) after the first programming and recovery process ($\epsilon_m = 25\%$, Method A); and (c) aligned PDLCL fabric prepared by electrospinning with rotating collector.

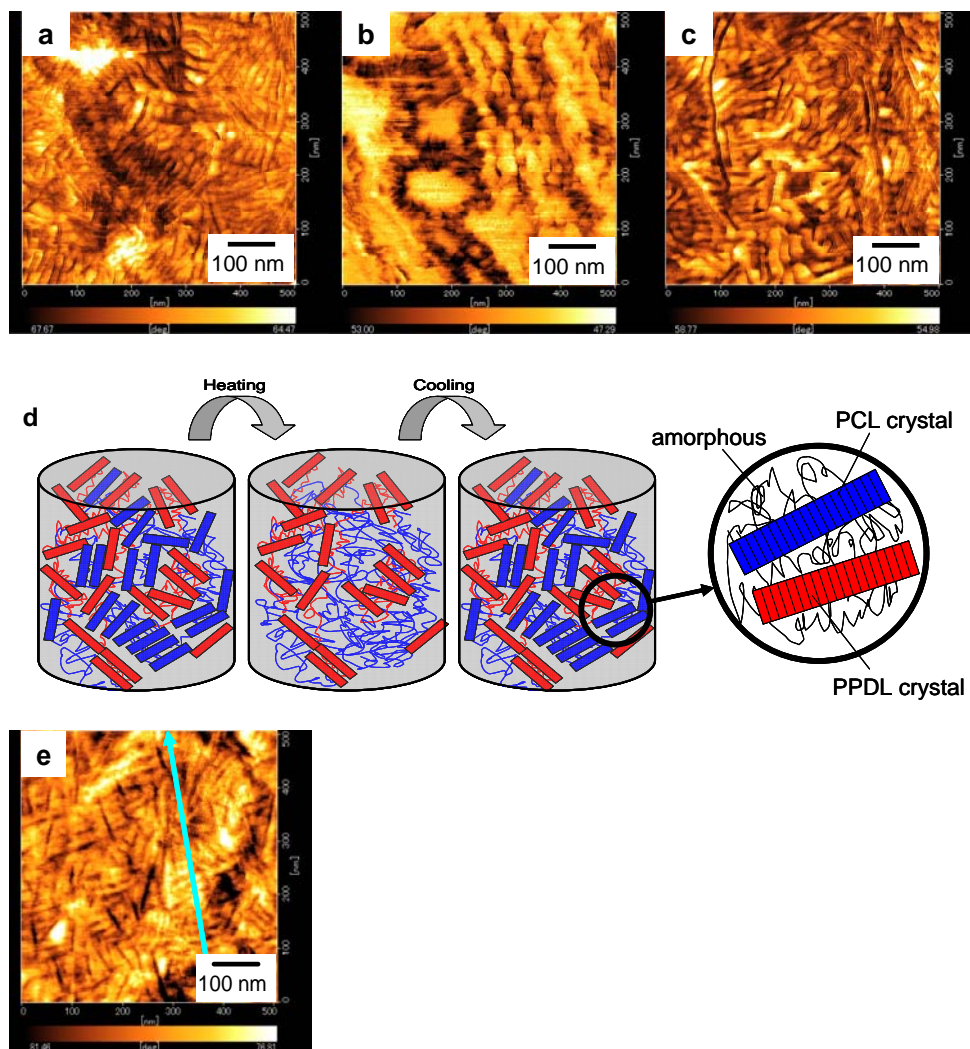


Figure 6. SPM phase mode images of the surface of electrospun PDLCL multiblock copolymer at different temperatures: (a) 25 °C; (b) 70 °C; and (c) 25 °C after heat treatment. (d) Schematic representation of the internal structures of the as-spun PDLCL multiblock copolymer. (e) SPM phase mode image of the surface of the electrospun PDLCL fiber taken at 25 °C after programming (elongation to $\epsilon_m = 25\%$ at $T_{high} = 60\text{ °C}$). Direction of the arrow in the image (e) represents fiber axis.

Table S1. Shape-memory properties of PDLCL fabrics with aligned fiber morphology obtained by the cyclic thermomechanical measurements with $T_{prog} = T_{high} = 60$ °C and $T_{low} = 40$ °C in three subsequent cycles with $\epsilon_m = 25\%$ according the test method (A)

Formatiert: Schriftartfarbe:
Automatisch

Cycle No.	Method A		
	ϵ_m [%]	$R_f(N)$ [%]	$R_r(N)$ [%]
	25	84	66
2	25	83	88
3	25	84	90

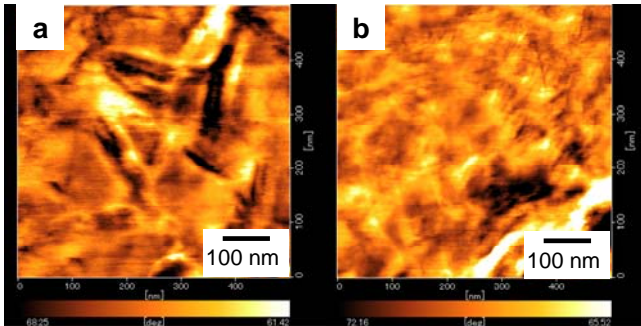


Figure S1. SPM phase mode images of the surface of (a) solvent casted and (b) spin coated PDLCL multiblock copolymer at 25 °C. The cast film and spin coated film were prepared on the glass plate and silicon wafer from 10 wt% and 2 wt% PDLCL/chloroform solutions, respectively.

Formatiert: Schriftartfarbe:
Automatisch